Proceedings of Computational Engineering Conference JSCES
Vol. 28, 2023 May

Evolution process of toe sliding failure of a dip slope model lying on a bedding plane with toe support

Wongchana Pongsakorn[1)] and Pipatpongsa Thirapong[2)]

1) Ph.D. Student (C1-2-236, Nishikyo-ku, Kyoto, 615-8540, Japan, E-mail: wongchana.pongsakorn.62y@st.kyoto-u.ac.jp)

2) Associate Professor (C1-2-234, Nishikyo-ku, Kyoto, 615-8540, Japan, E-mail: pipatpongsa.thirapong.4s@kyoto-u.ac.jp)

This study investigates the evolution process of toe sliding failure in a dip slope model with toe support on a bedding plane using physical model experiments and particle image velocimetry (PIV) analysis. The results show that the toe angle is a crucial factor in slope stability and significantly influences the failure mechanism and mode of deformation. The analysis reveals that a reduction in the toe angle results in a shift from fore-thrust failure to toe sliding failure, indicating the significant role of this parameter in slope stability. The findings provide valuable insights into the factors influencing the evolution of toe sliding failure and can help accurately evaluate slope stability analysis.

Key Words: *Toe slope, Dip slope, Particle image velocimetry*

1. INTRODUCTION

The stability of slopes is an important concern in many engineering and geological applications, as slope failures can lead to property damage, loss of life, and significant economic costs. One common failure mechanism of slopes is toe sliding, which occurs when the toe of the slope begins to slide along a support surface, leading to instability and collapse. While the mechanisms of toe sliding have been studied extensively in the literature, there is still much to learn about the evolution process of this failure mode, especially for slopes lying on a bedding plane with toe support. Understanding this process is critical for designing and maintaining stable slopes in various natural and man-made environments.

In this study, we investigate the evolution process of toe sliding failure in a dip slope model lying on a bedding plane with toe support, using physical experiments and particle image velocimetry (PIV). We focus on the influence of the toe angle and other key parameters on the failure mechanism and mode of deformation of the slope and discuss the implications of our findings for slope stability analysis.

2. METHODOLOGY

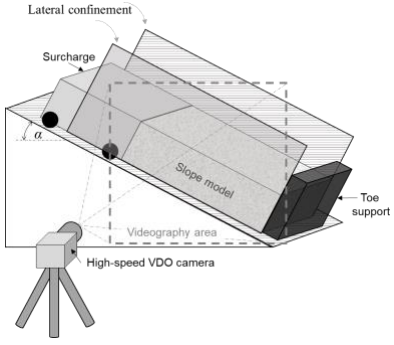

Fig. 1 Schematic diagram of the experimental setup

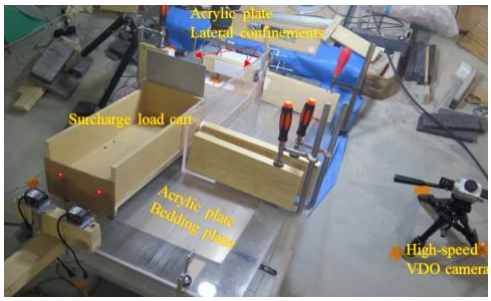

Fig. 2 Experimental installation

A physical model at 1G was utilized to investigate the failure mechanism associated with surcharge loading-induced instability of a slope on a bedding plane. As shown in Fig. 1, the soil slope model was constructed on a bedding plane and toe support, with lateral confinements employed based on the methodology proposed by Pipatpongsa et al. (2022) [1]. Additionally, a surcharge was installed at the top of the slope to induce failure by applying additional weight. A high-speed camera was used to record the slope motion during failure, and the videography area covered the entire slope model to facilitate movement analysis in subsequent stages of the study.

For the slope stability experiment, silica sand no.6 was used as the material for constructing the slope models through the compaction method mentioned below: Acrylic plates were installed as the bedding plane and lateral supports, as shown in Fig. 2. In addition, toe support was covered by Teflon material. The surcharge load cart was designed specifically to enable the addition of metal weights, as depicted in Fig. 2. The basic properties of silica sand no.6 and interface properties on acrylic plates are presented in Table 1.

Once the construction of the slope model was completed, a surcharge load cart was installed on the top of the slope. The

© 一般社団法人日本計算工学会

surcharge weight was incrementally increased by adding metal weights until the slope reached its collapse point. In this study, 12 slope models were tested under varying geometric conditions, as shown in Table 2. The research objective focuses on the effect of the geometry of the toe support. Therefore, slope angles of 30º and 50º were studied, considering a change in the toe angle. Fig. 3 illustrates the perspective captured by the high-speed camera, including the slope angle (α), toe angle (β), thickness, and length.

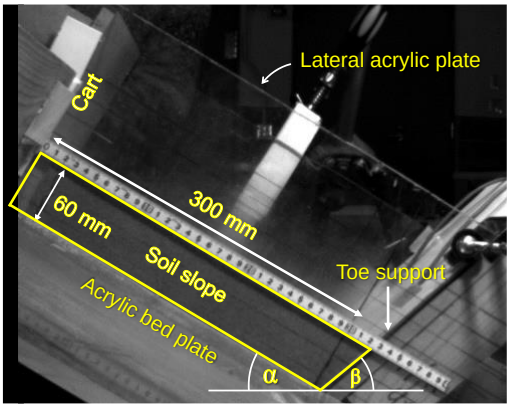

Fig. 3 Slope model compacted on bedding plane and being confined by two lateral supports

Table 1 Basic properties of Silica sand no.6

Bulk density (γ)	13.68 kN/m^3
Water content (w)	10.0%
Friction angle (ϕ)	33.2°
Apparent cohesion (c)	0.57 kPa
Friction angle of roller cart (ϕ_r)	6.1°
Interface friction angle of humid sand on acrylic plate (ϕ_i)	29.4°
Interface adhesion of humid sand on acrylic plate (c_i)	0.26 kPa
Interface friction angle of humid sand on Teflon plate (ϕ_t)	21.0°
Interface adhesion of humid sand on Teflon plate (c_t)	0.03 kPa

Table 2 Geometry conditions of slope model

Test №	Thickness (mm)	Length (mm)	Breadth (mm)	Slope angle α (°)	Toe angle β (°)
A1 A2 A3	60	300	209	30	60
B					40
C					20
D					0
E1 E2				50	40
F					20
G1 G2					0
H					-20

3. PARTICLE IMAGE VELOCIMETRY

During the experiment, a high-speed camera with a resolution of 800×600 pixels and a frame rate of 200 fps was employed to capture the movement of the slope model from one side during the loading process. However, due to the limitations of visual observation, it was difficult to analyze the recorded video. To address this challenge, particle image velocimetry (PIV) was proposed as a technique to accurately analyze the movement of the slope. In this study, the movement of the slope was analyzed using the PIVlab software, which is a MATLAB application specifically designed for particle image velocimetry (PIV) analysis [2]. It has been demonstrated by Senatore et al. (2013) that PIVlab is a reliable tool that can be utilized for granular material analysis. The results of the experiment confirm that it is possible to accurately calculate soil deformation characteristics without the use of markers. Soil velocity measurements obtained from PIV analysis can be used to calculate the strain fields [3].

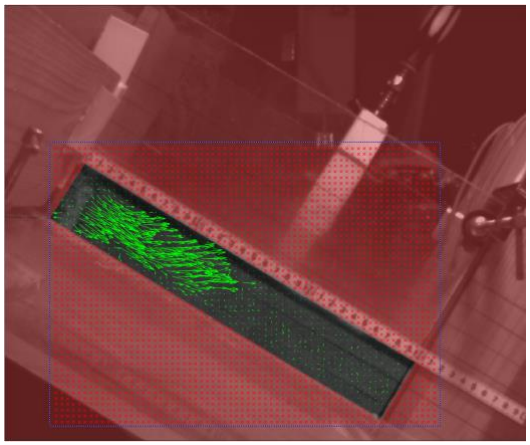

Fig. 4 Velocity vectors from PIV analysis for A2

Fig. 4 illustrates an example of the vector velocity results for test A2 obtained from the PIV analysis. The velocity vectors are represented by green arrows and define both the direction and magnitude of the movement for each frame. To isolate the soil model in the image analysis, a mask (red zone) was used to eliminate other areas. PIV algorithms typically compare groups of pixels within a specific area called an "interrogation window" (IW). The optimal size of the IW and frame rate can vary depending on the experimental conditions. Senatore et al. (2013) recommend an average of 10 particles per IW to maximize the accuracy of the PIV algorithm. They also suggest that the particle displacement should not exceed 25% of the IW length to avoid errors in velocity measurement. In this study, IW sizes of 64, 32, and 16 were used as the analysis settings. To further improve the accuracy of PIV analysis, these 3 passes were used in multi-pass PIV, where the results of each pass were used to improve the estimation of IW in the next pass.

© 一般社団法人日本計算工学会

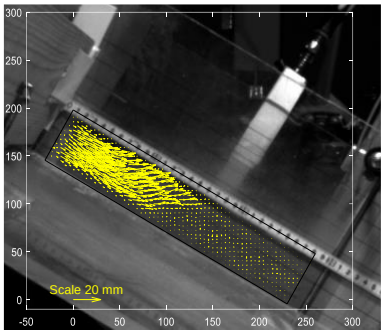

(a) Test no. A1

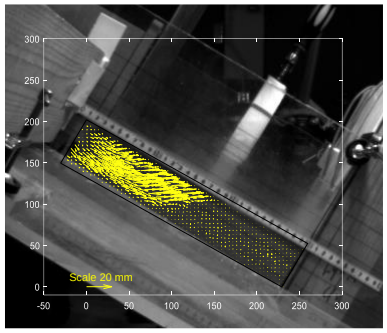

(b) Test no. A2

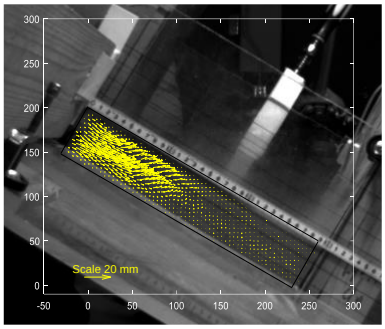

(c) Test no. A3

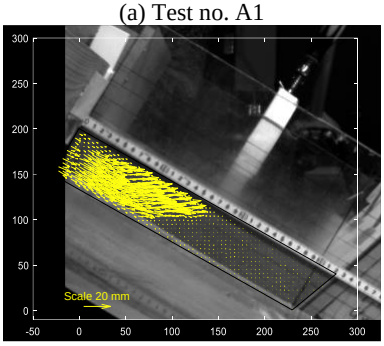

(d) Test no. B

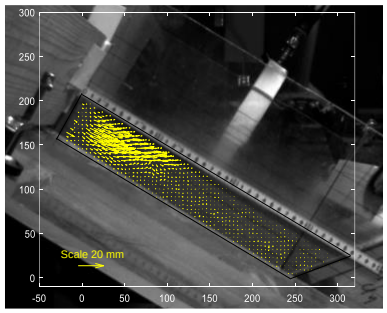

(e) Test no. C

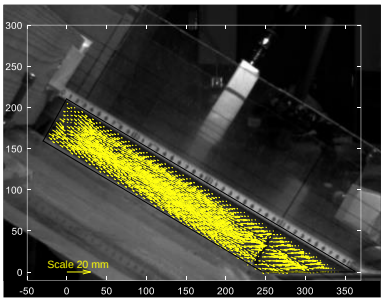

(f) Test no. D

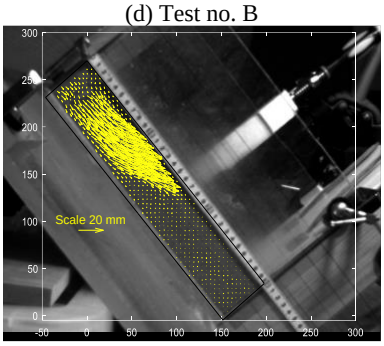

(g) Test no. E1

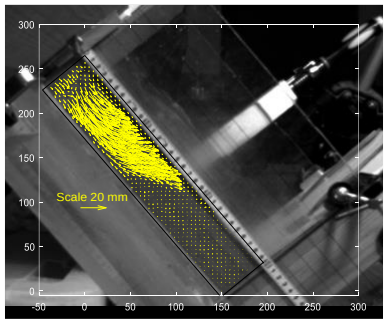

(h) Test no. E2

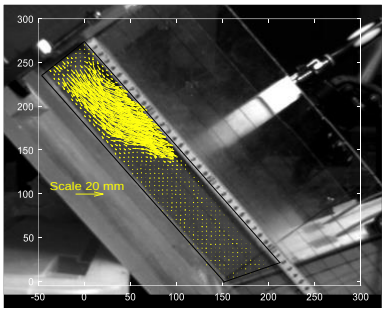

(i) Test no. F

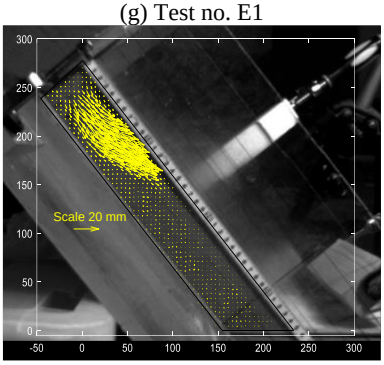

(j) Test no. G1

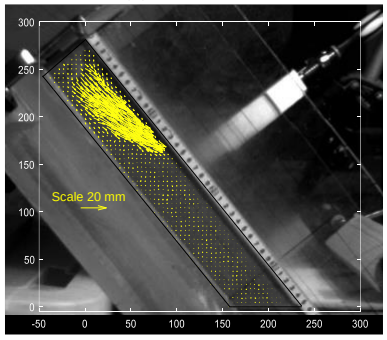

(k) Test no. G2

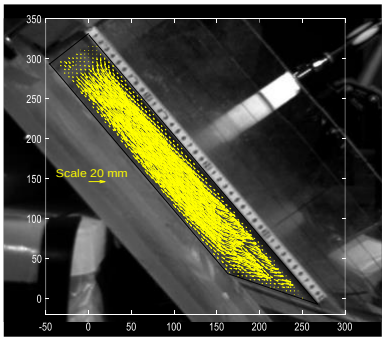

(l) Test no. H

Fig. 5 PIV analyses for surcharge displacement 2 centimeters

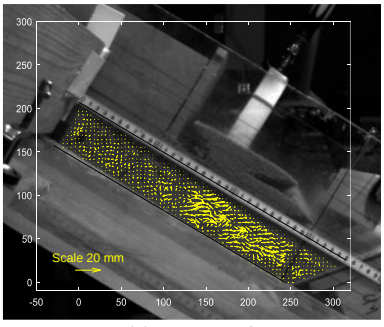

(a) Test no. C

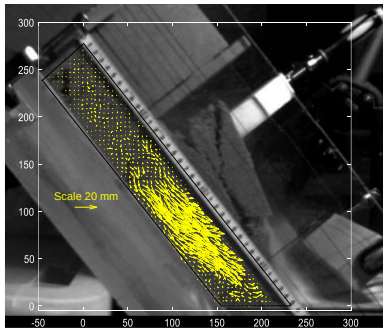

(b) Test no. G1

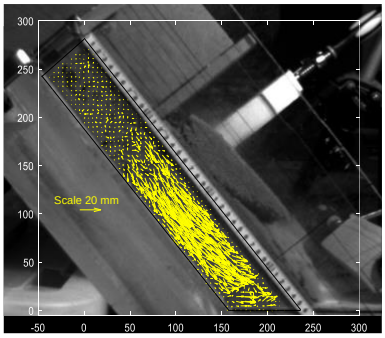

(c) Test no. G2

Fig. 6 PIV analyses for surcharge displacement 10 centimeters

© 一般社団法人日本計算工学会

4. RESULTS

Fig. 5 illustrates the displacement vectors of the slope movement, where slope angles of 30° and 50° were investigated while taking into account a variation in the toe angle. The results from PIV analysis show the evolution process of toe sliding failure. The movement of the surcharge was fixed by 2cm down the slope, to ensure consistency and display the results under the same failure condition. Tests A1, A2, and A3 were performed with identical geometry conditions, specifically slope angles (α) of 30° and toe angles (β) of 60°. The tests resulted in failure due to the fore-thrust failure mechanism during the loading process, as depicted in Fig. 5(a) to 5(c). Similarly, tests B and C were conducted with reduced toe angles of 40° and 20°, respectively, and the observed failure mechanism was fore-thrust failure.

Regarding the slope angle of 50°, tests E1 and E2 were conducted under identical geometry conditions (α=50° and β=40°) and resulted in failure due to the fore-thrust failure mechanism. Additionally, tests F and G were carried out with reduced toe angles (β) of 20° and 0°, respectively, and the failure mechanism observed was fore-thrust failure.

Tests A, B, E, and F exhibited fore-thrust failure throughout the entire loading process, while in tests C and G, the failure mechanism shifted from fore-thrust to toe sliding once the surcharge loading displacement exceeded 10 cm (see Fig. 6).

On the other hand, the results of the last test (D and H) in Fig. 5(f) and Fig. 5(l) show significant deformation along with slope due to sliding at toe, indicating that the toe angle plays a crucial role in the overall stability of the slope.

5. DISCUSSION

Based on the results of the PIV analysis, it is clear that the toe angle is a critical factor in slope stability, as it significantly influences the failure mechanism and mode of deformation of the slope. Tests A, B, and F consistently showed fore-thrust failure until the end of the loading process, indicating the role of toe angle in slope stability. Conversely, tests C and G exhibited a change in the failure mechanism from fore-thrust failure to toe-sliding as surcharge loading displacement exceeded 10 cm. Additionally, tests D and H experienced significant deformation due to toe sliding failure, further highlighting the significance of the toe angle in slope stability. These results suggest that the toe angle should be considered as an important parameter in slope stability analysis and design. The summary of results is illustrated in Table 3.

To analyze the failure mechanisms based on the experimental results, it is important to note that when the sum of the slope angle (α) and the toe angle (β) equals 90°, the direction of the surcharge loading will be perpendicular to the toe support. In such cases, the reaction force acting on the slope will be the passive earth pressure. A reduction in toe angle has the effect of decreasing passive earth pressure, while simultaneously increasing the interface friction between the soil and toe support. A slope is susceptible to fore-thrust failure if the sum of the slope angles (α) and toe angle (β) is high. Conversely, if a sum of α and β is slow, the slope is prone to toe-sliding failure.

Table 3 Experimental results of failure condition

Test №	Slope angle α (°)	Toe angle β (°)	Failure condition
A1	30	60	Fore-thrust
A2			Fore-thrust
A3			Fore-thrust
B		40	Fore-thrust
C		20	Fore-thrust and Toe-sliding
D		0	Toe sliding
E1	50	40	Fore-thrust
E2			Fore-thrust
F		20	Fore-thrust
G1		0	Fore-thrust and Toe-sliding
G2			Fore-thrust and Toe-sliding
H		-20	Toe sliding

6. CONCLUSION

In conclusion, this study presents physical model experiments that investigate the failure mechanism associated with surcharge loading-induced instability of a slope on a bedding plane. The utilization of particle image velocimetry (PIV) analysis enables accurate measurement and analysis of the soil deformation characteristics during the experiment. The results emphasize the critical role of the toe angle in slope stability, as it significantly influences the failure mechanism and mode of deformation of the slope. The findings demonstrate that a reduction in the toe angle leads to a shift from fore-thrust failure to toe sliding failure, indicating the importance of this parameter in slope stability.

ACKNOWLEDGMENT: This work was supported by EGAT (Electricity Generating Authority of Thailand).

REFERENCES

[1] Pipatpongsa, T. et al.: Stability analysis of laterally confined slope lying on inclined bedding plane, *Landslides*, Vol.19(8), pp.1861-1879, 2022.

[2] Thielicke, W. et al.: Particle Image Velocimetry for MATLAB: Accuracy and enhanced algorithms in PIVlab, *Journal of Open Research Software*, Vol.9(1), 2021.

[3] Senatore, C. et al.: Design and implementation of a particle image velocimetry method for analysis of running gear–soil interaction, *Journal of Terramechanics*, Vol.50(5-6), pp.311-326, 2013.

© 一般社団法人日本計算工学会